squares with the computer program CORELS (*10*). The positional parameters of individual atoms were then refined subject to stereochemical restraints by using the subcell data (*6*). The positions of missing side-chain atoms and those of the benzamidine and calcium were determined from the subcell difference electron density map computed from the refined model. A model of the full crystallographic asymmetric unit in the correct $P2_12_12_1$ unit cell was then constructed by adding a replicate of the trypsin molecule translated by 46 Å along the *b* and 32 Å along *c*. The full model was refined in three stages. In each stage the model was refit to a difference Fourier map computed with the coefficients $(2F_{obs} - F_{calc})$. Strong peaks in the electron density in positions consistent with hydrogen bond contacts to the protein or other established solvent positions were included in the model as ordered solvent. Next, the positional and thermal parameters of all atoms were refined by iterations of restrained crystallographic least squares, with data in the resolution range 6 Å $\leq d \leq$ 2.3 Å. Refinement was stopped when further cycles failed to reduce the crystallographic *R* factor and when the mean shift in coordinate positions was less than 0.05 Å. Refined coordinates were then used to compute phases for a new electron map to be used in the next stage of manual refitting. After the third stage (*R* factor = 0.18), examination of the electron density failed to reveal errors or ambiguity in main- or side-chain positions, although the side chains of six residues located at the surface of the molecules were disordered and could not be defined. Up to this point, side-chain atoms for His^{57}, Asn^{102}, or Ser^{195} had been excluded from the model. A difference electron density map $(F_{obs} - F_{calc})$ revealed strong and well-ordered density for the Asn^{102} and Ser^{195}, but the His^{57} residue appeared to be statistically disordered (Fig. 2, top) (*11*).

10. J. L. Sussman, S. R. Holbrook, G. M. Church, S. H. Kim, *Acta Crystallogr.* **A32**, 311 (1976).
11. The possibility that one or other of the peaks are artifactual was tested by independent refinement of two alternative models: one with His^{57} fit to the stronger, internal density and the second with His^{57} fit to the external density. In each model the His^{57} atoms were assigned full occupancy and side-chain positions for Asn^{102} and Ser^{195} were included. Each model was subjected to restrained crystallographic refinement by varying the thermal and positional parameters of all atoms. Subsequently, a difference Fourier map $(F_{obs} - F_{calc})$ was computed for each model with the use of the refined positional and thermal parameters for all of the atoms in the respective models. In both cases, residual electron density appeared at the alternative histidine site. Again, the observed density peaks were contiguous with the Cβ atom of His^{57} and thus could not be interpreted as ordered water molecules. The relative occupancy of the two histidine positions and the total occupancy of both positions relative to other histidine side chains was estimated by integration of difference electron density at all of the histidine side-chain positions in one of the trypsin molecules in the asymmetric unit. The difference Fourier map $(F_{obs} - F_{calc})$ used in the integration was computed from a model in which the side-chain atoms of all four histidine residues (at sequence positions 40, 57, 70, and 87) were removed from the coordinate set of one molecule. Integration was performed manually by summing over all grid points within 2.0 Å of histidine atomic positions that had electron density at least one standard deviation greater than the background density. After normalization the apparent relative integrated difference densities at the histidine side-chain positions were: His^{40}, 0.87; His^{57}, 0.60; His^{70}, 0.79; and His^{87}, 1.0. All but His^{57} are well ordered, so the range in integrated densities reflects thermal motion and experimental error. The sum of the density over the two His^{57} side-chain sites is lower than the mean density of the well-ordered histidine side chains, but is consistent with the high B factors of His^{57} atoms at both positions. The relative occupancy of the alternative His^{57} positions was estimated by integrating the difference density at the Nδ1 and Cε1 atoms of the gauche conformer and the Cδ2 and Nε2 atoms of the trans conformer and by taking the ratio of the integrated densities for the two positions. The remaining histidine atoms were not included in the integration because the resolution of the data set did not allow the densities of the two conformers to be resolved at those positions.

Final refined positional and thermal parameters for both trans and gauche conformers were determined by refining an atomic model in which both conformers were simultaneously included. Side-chain atoms of the gauche conformer were assigned occupancies of 0.67 and atoms of the trans isomer were assigned occupancies of 0.33 based on the estimate derived from the integration described above (*12*). After three final cycles of refinement of all thermal and positional parameters of both trypsin monomers in the asymmetric unit, the crystallographic *R* factor was 0.161.

12. A modified version of PROTIN (obtained from J. Smith) does not generate restraints between alternate side-chain positions of a statistically disordered residue. This allows refinement of two conformations of an amino acid simultaneously.
13. W. Bode and P. Schwager, *J. Mol. Biol.* **98**, 693 (1975).
14. R. Henderson, *ibid.* **54**, 341 (1970).
15. An upper estimate of the mean error in atomic position is 0.25 Å. It was obtained by an analysis of the variation of crystallographic *R* factor as a function of resolution (*16*).
16. V. Luzatti, *Acta Crystallogr.* **6**, 142 (1953).
17. A. A. Kossiokoff and S. A. Spencer, *Biochemistry* **20**, 6462 (1981).
18. M. Krieger *et al.*, *ibid.* **15**, 3458 (1976).
19. M. N. G. James, A. R. Sielecki, G. D. Brayer, L. T. Delbaere, C. A. Bauer, *J. Mol. Biol.* **144**, 43 (1980).
20. P. H. Morgan *et al.*, *Proc. Natl. Acad. Sci. U.S.A.* **69**, 3312 (1972).
21. A. A. Kossiakoff *et al.*, *Biochemistry* **16**, 654 (1977); H. Fehlhammer, W. Bode, R. Huber, *J. Mol. Biol.* **111**, 415 (1977).
22. J. L. Chambers *et al.*, *Biochem. Biophys. Res. Commun.* **59**, 70 (1974).
23. M. O. Jones and R. M. Stroud, *Biochemistry*, in press.
24. D. M. Blow *et al.*, *Nature (London)* **221**, 337 (1969).
25. C. S. Craik *et al.*, *J. Biol. Chem.* **259**, 14255 (1984).
26. The coordinates were obtained from the Protein Data Bank at Brookhaven National Laboratory.
27. We thank J. Sadowsky, C. Neilsen, and E. Goldsmith for assistance with Area Detector data collection and processing and B. Montfort for assistance with crystallographic refinement calculations. We gratefully acknowledge grant support from NIH: AM31507 to S.R.S., GM24485 to R.M.S., and AM26081 to R.J.F.; from NSF: DMB8608086 to C.S.C. and PCM830610 to W.J.R.; a Bristol Meyer grant of Research Corporation and a CCRC grant to C.S.C. The coordinates of the D 102 N trypsin structure at *p*H 6 have been submitted to the Protein Data Bank at Brookhaven National Laboratory.

29 September 1986; accepted 29 May 1987

The Catalytic Role of the Active Site Aspartic Acid in Serine Proteases

CHARLES S. CRAIK, STEVEN ROCZNIAK,* COREY LARGMAN,† WILLIAM J. RUTTER

The role of the aspartic acid residue in the serine protease catalytic triad Asp, His, and Ser has been tested by replacing Asp^{102} of trypsin with Asn by site-directed mutagenesis. The naturally occurring and mutant enzymes were produced in a heterologous expression system, purified to homogeneity, and characterized. At neutral *p*H the mutant enzyme activity with an ester substrate and with the Ser^{195}-specific reagent diisopropylfluorophosphate is approximately 10^4 times less than that of the unmodified enzyme. In contrast to the dramatic loss in reactivity of Ser^{195}, the mutant trypsin reacts with the His^{57}-specific reagent, tosyl-L-lysine chloromethylketone, only five times less efficiently than the unmodified enzyme. Thus, the ability of His^{57} to react with this affinity label is not severely compromised. The catalytic activity of the mutant enzyme increases with increasing *p*H so that at *p*H 10.2 the k_{cat} is 6 percent that of trypsin. Kinetic analysis of this novel activity suggests this is due in part to participation of either a titratable base or of hydroxide ion in the catalytic mechanism. By demonstrating the importance of the aspartate residue in catalysis, especially at physiological *p*H, these experiments provide a rationalization for the evolutionary conservation of the catalytic triad.

SERINE PROTEASES FUNCTION IN many biological systems to hydrolyze specific polypeptide bonds. Trypsin, a well-studied member of this family, catalyzes the hydrolysis of peptide and ester substrates that contain lysyl or arginyl side chains. Serine proteases have the triad of residues Asp^{102}, His^{57}, and Ser^{195} at the active site (chymotrypsin numbering system). X-ray crystallographic studies reveal that these three residues are in close proximity, which suggests they may serve as a functional interacting unit responsible for bond formation and cleavage during catalysis (*1*). Numerous chemical and physical studies indicate that Ser^{195} and His^{57} play crucial roles in catalysis. For example, selective reaction of Ser^{195} with diisopropylfluor-

C. S. Craik, Departments of Pharmaceutical Chemistry and of Biochemistry and Biophysics, University of California, San Francisco, San Francisco, CA 94143-0446. S. Roczniak, C. Largman, W. J. Rutter, Hormone Research Institute and Department of Biochemistry and Biophysics, University of California, San Francisco, San Francisco, CA 94143-0448.

*Present address: NutraSweet Company, Mount Prospect, IL 60056.
†Present address: Veterans Administration Hospital, Martinez, CA 94553, and Departments of Internal Medicine and Biological Chemistry, University of California, Davis, CA 95616.

ophosphate (DFP) (*2*) or modification of the His^{57} of trypsin with tosyl-L-lysine chloromethyl ketone (TLCK) (*3*) blocks catalytic activity. The collective data suggest that substrate hydrolysis is facilitated through nucleophilic attack by the Ser^{195} hydroxyl oxygen on the carbonyl carbon of the substrate. Concomitantly the hydroxyl proton of the serine can be transferred to the imidazole of His^{57} and subsequently donated to the resulting leaving group (alcohol or amine) in the reaction. The remaining acyl enzyme intermediate is hydrolyzed by a mechanism that is the reverse of its formation except that water instead of Ser^{195} serves as the nucleophile. The role of the buried carboxylate of Asp^{102} in the catalytic process remains to be clarified experimentally.

The geometric relation of the amino acids in the catalytic triad led to the postulate that Asp^{102} serves in concert with the histidine imidazole group to transfer the proton from the serine in a charge-relay mechanism (*4*). However, ^{15}N nuclear magnetic resonance (NMR) studies (*5*) showed that the Asp^{102} and the His^{57} moieties displayed normal pK_a values (K_a is the ionization constant); this is incompatible with the implications of the charge-relay mechanism (*6*). Furthermore, neutron diffraction and ^1H NMR studies of the imidazole nitrogens in the resting state of the enzyme show that no proton transfer occurs from His^{57} to Asp^{102} (*7*). Asp^{102} may be involved in the stabilization of the imidazolinium intermediate and the orientation of the correct tautomer of His^{57} relative to Ser^{195} and the substrate (*8*). However, a test of the function of Asp^{102} by selective chemical modification, has not been possible because it is inaccessible to chemical reagents under nondenaturing conditions. We have evaluated the catalytic role of Asp^{102} by replacing this residue with Asn. This eliminates the negative charge with little change in the van der Waals surface of the side-chain atoms (NH_2 versus OH).

Conversion of the Asp^{102} codon (GAC) to an Asn (AAC) codon within the rat anionic trypsinogen DNA (*9*) was accomplished by site-directed mutagenesis (*10*). The DNA that encodes the mutant enzyme was sequenced in its entirety to ensure that no inadvertent base changes were introduced during the mutagenesis procedure. The mutant enzyme $trypsin^{102}$ (Asp → Asn), referred to as D 102 N trypsin and the naturally occurring trypsin were expressed under the control of the simian virus 40 (SV40) early promoter (*11*) in stably transformed eukaryotic cell lines that secreted the zymogen form of the enzymes into the culture medium (*12*). D 102 N trypsin and trypsin were purified to homogeneity and crystallinity by a combination of ion-exchange and affinity chromatography techniques. Trypsin isolated from this expression system displayed physical and catalytic properties identical to trypsin purified from the rat pancreas. In contrast, D 102 N trypsin exhibited dramatically different catalytic activity.

The activities of trypsin and D 102 N trypsin toward various substrates and inhibitors are compared in Table 1. At neutral *p*H the catalytic efficiency of D 102 N trypsin as measured by its ability to hydrolyze the ester substrate *N*-benzyloxycarbonyl-L-lysine thiobenzyl ester (Z-Lys-S-Bzl) is severely compromised (k_{cat} or k_{cat}/K_m values are $\sim 10^4$ times lower than that of trypsin; k_{cat} is the catalytic rate constant and K_m is the

Table 1. Ratios of activity for trypsin and D 102 N trypsin. Assays for Z-Lys-S-Bzl were performed at *p*H 7.15 and 10.18 (see legend to Fig. 1 for a description of the experimental conditions). Values for $k_{obs}/[I]$ with DFP were determined by the method of Kitz and Wilson (*24*). Standard conditions (*25*) were used except when the initial DFP concentration was 10 m*M* in assays with D 102 N trypsin at *p*H 10.03; background hydrolysis of DFP was relatively rapid and enzymatic activity at infinite times did not equal zero. In this case the $k_{obs}/[I]$ value (where [I] is the concentration of inhibitor) was determined by the method of Yosgimura *et al.* (*26*). Values of $k_{obs}/[I]$ from assays with trypsin were calculated to be $790 \pm 80 M^{-1}$ min^{-1} (*p*H 7.96) and $980 \pm 70 M^{-1}$ min^{-1} (*p*H 10.03). In assays with D 102 N trypsin these values were $0.070 \pm 0.008 M^{-1}$ min^{-1} (*p*H 7.96) and $0.098 \pm 0.019 M^{-1}$ min^{-1} (*p*H 10.03). Titrations with MUGB were followed at 360 nm on a Perkin-Elmer LS5 spectrofluorometer and performed in triplicate in 50 m*M* Hepes buffer, *p*H 7.5, that contained 2 μ*M* MUGB. Titrations of trypsin were complete in 2 seconds (the minimum detection time of the fluorometer) or less when enzyme concentrations ranged from 50 n*M* to 400 n*M*. Approximately 17 minutes elapsed before a molar equivalence of MUGB reacted with 400 n*M* D 102 N trypsin. Values for $k_{obs}/[I]$ with TLCK were determined by the method of Kitz and Wilson (*24*); standard conditions were used (*27*). $k_{obs}/[I]$ values from assays with trypsin were calculated to be $760 M^{-1}$ min^{-1} (*p*H 7.16) and $387 M^{-1}$ min^{-1} (*p*H 8.77). In assays with D 102 N trypsin these values were $149 M^{-1}$ min^{-1} (*p*H 7.16) and $28 1 M^{-1}$ min^{-1} (*p*H 8.77). The instability of TLCK and MUGB at alkalaine *p*H values precluded these assays at higher *p*H values.

Ligand	Kinetic constant	Relative activity	
		Neutral *p*H	Alkaline *p*H
Z-Lys-S-Bzl	k_{cat}	4,400	18
Z-Lys-S-Bzl	k_{cat}/K_m	11,300	152
DFP	$k_{obs}/[I]$	11,300	10,000
MUGB	v_{titr}	>500	
TLCK	$k_{obs}/[I]$	5.1	1.4

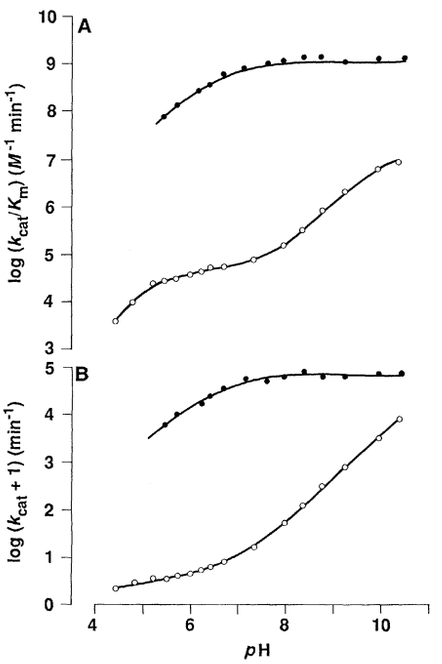

Fig. 1. Profile of activities for trypsin and D 102 N trypsin-catalyzed hydrolysis of Z-Lys-S-Bzl. (**A**) Plot of log(k_{cat}/K_m) versus *p*H and (**B**) plot of log k_{cat} versus *p*H, for trypsin (●), and D 102 N trypsin (○). Assays were performed at 25°C in 50 m*M* Mes [2-(*N*-morpholino)ethanesulfonic acid], Mops, or Taps buffers, *p*H 4.43 to 8.77, or 50 m*M* glycine, *p*H 9.25 to 10.18, that contained 0.1*M* NaCl and 1 m*M* $CaCl_2$. Stock solutions of Z-Lys-S-Bzl and 4,4′-dithiodipyridine were prepared in water and dimethylformamide, respectively. The *p*H of all reactions was determined immediately after reaction. To a cuvette that contained 0.97 ml of the assay solution was added 10 μl of a 25 m*M* solution of 4,4′-dithiodipyridine (final concentrations: 250 μ*M* 4,4′-dithiodipyridine and 1% dimethylformamide) and 10 μl of a Z-Lys-S-Bzl stock solution. The concentration of substrate ranged from ten times greater than to ten times less than the K_m of the enzyme. After the background rate of hydrolysis was measured spectrophotometrically (Beckman DU-7) at 324 nm, 10 μl of an enzyme stock solution (in the case of trypsin, diluted in 0.5 mg per milliliter of bovine serum albumin) was added and the initial rate of hydrolysis was measured. At *p*H values greater than 9.25, for which the background hydrolysis was substantial (up to 2% Z-Lys-S-Bzl hydrolyzed per minute), a reference cell that contained substrate and 4,4′-dithiodipyridine was used during kinetic measurements. In all of the assays the initial rates were measured from data for the initial 5 to 10% of the hydrolysis of substrate. Z-Arg-S-Bzl was not used as substrate because this compound shows a background hydrolysis rate 20 times greater than that for Z-Lys-S-Bzl at alkaline *p*H (*14*). Substrate and enzyme concentration determinations were performed with standard procedures (*29, 30*). Values for k_{cat} and K_m parameters from all assays were derived by a program that performed a weighted linear and nonlinear squares regression analysis of data by using the Lineweaver-Burk and Michaelis-Menton equations, respectively (*31*). Double reciprocal plots of the data were linear in all cases. Values of pK_a and k_{enz} were determined by the program MULTI (*32*) which performs a nonlinear squares analysis of the data.

Michaelis constant). However, the relative activity of the mutant enzyme progressively increases with increasing *p*H values. To determine the relative reactivity of Ser^{195} and His^{57} both enzymes were treated with the specific active site–directed reagents DFP and TLCK. The inhibition of D 102 N trypsin by DFP, which is specific for Ser^{195}, is approximately four orders of magnitude slower than that of trypsin at both *p*H 8.0 and *p*H 10.0. The active site titrant 4-methylumbelliferyl - *p* - guanidinobenzoate (MUGB) (*13*) also reacts with D 102 N trypsin at a rate at least 500-fold slower than with trypsin at *p*H 7.5. These data suggest that the nucleophilicity of Ser^{195} is dependent on the negative charge of Asp^{102}.

The substrate analog TLCK reacts specifically with His^{57}, presumably because the binding pocket of the substrate positions the reactive chloromethyl-ketone group adjacent to His^{57}. In contrast to the large decreases in activity monitored with DFP and MUGB, TLCK is five times less reactive with D 102 N trypsin than with trypsin at neutral *p*H (*p*H 7.2) and one and a half times less reactive at more alkaline *p*H (*p*H 8.8). Thus the active site reacts virtually normally with the affinity reagent. The differential effect of the Asp to Asn substitution on the inhibition of D 102 N trypsin by DFP and TLCK may be due to differences in the proximity of the reactive groups of the inhibitors and the enzyme. However, a more likely explanation is that the imidazole of His^{57} in D 102 N trypsin is not in the correct tautomeric state for removal of the Ser^{195} proton and thereby reduces the reactivity of the enzyme to DFP. However, His^{57} can still react with the chloromethyl ketone moeity of TLCK and thereby inhibit the enzyme.

The modified and unmodified enzymes exhibit different *p*H activity profiles for the ester substrate (Table 1 and Fig. 1). Similar data have been obtained with peptide substrates (*14*). In agreement with studies on bovine cationic trypsin (*15*), rat anionic trypsin shows a sigmoidal dependence of activity (pK_a = 6.8) with maximal k_{cat} and k_{cat}/K_m values of 7498 ± 254 min^{-1} and 1.20 ± 0.28 × $10^9 M^{-1}$ min^{-1}, respectively (*16, 17*). The rat enzyme resembles porcine elastase (*18*) but differs from bovine trypsin in being alkaline stable. The dominant effect of the Asp to Asn mutation is on k_{cat}. The K_m values of the two enzymes are similar at any given *p*H value. The D 102 N trypsin activity is dramatically lower (~10^4 times as measured by k_{cat} or k_{cat}/K_m) than trypsin activity at neutral *p*H values; however, it increases progressively at alkaline *p*H values from the low value at neutral *p*H to values

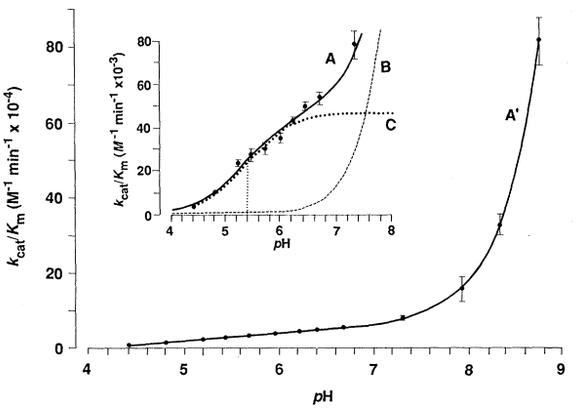

Fig. 2. The *p*H dependence of the kinetic parameter k_{cat}/K_m of D 102 N trypsin–catalyzed hydrolysis of Z-Lys-S-Bzl. The points correspond to the experimentally derived k_{cat}/K_m values. Curve A′ is derived from substituting the calculated rate and equilibrium constants k_{OH}, k_{enz}, K_1, and K_2 into Eq. 1. Values for k_{OH} and k_2 were determined from assays performed from *p*H 8.36 to 10.18 where it is assumed that $K_1 >> [H^+]$ and $k_{OH}[OH^-] >> k_{enz}$. Equation 1 can then be simplified and rearranged to describe a straight line: $(k_{cat}/K_m)[H^+] = -K_2(k_{cat}/K_m) + (10^{-14})k_{OH}$. Linear regression of this line yields k_{OH} and K_2 values of 1.45 ± 0.12 × $10^{11} M^{-2}$ min^{-1} and 1.21 ± 0.30 × $10^{-10} M$, respectively. Values of K_1 and k_{enz} were determined from assays performed from *p*H 4.43 to 7.33 where $[H^+] >> K_2$. By using the k_{OH} value determined above, Eq. 1 can again be simplified to a linear form: $[k_{cat}/K_m)[H^+] - 1.45 \times 10^{-3}]/[H^+] = 1/K_1[1.45 \times 10^{-3} - (k_{cat}/K_m)[H^+]] + k_1$. Linear regression analysis of this line yields k_{enz} and K_1 values of 4.78 ± 0.22 × $10^4 M^{-1}$ min^{-1} and 3.67 ± 0.32 × $10^{-6} M$, respectively. Inset: Plot of k_{cat}/K_m versus *p*H from *p*H 4.43 to 7.33. Curve A is the same as described above. Curve B describes the contribution to the catalytic rate of D 102 N trypsin that depends on $[OH^-]$: $k_{OH}[OH^-]/(1 + K_2/[H^+])$. Curve C describes the contribution to the catalytic rate of D 102 N trypsin independent of $[OH^-]$ detected at lower *p*H values: $k_1/[1 + ([H^+]/K_1) + (K_2/[H^+])]$. Note that curve A is the sum of curves B and C. The dotted line perpendicular to the abscissa is the pK_a of the mutant enzyme calculated from the inflection point of the activity profile.

Table 2. Values for k_{OH}, k_{enz}, and pK_a derived from the D 102 N trypsin–catalyzed hydrolysis of Z-Lys-S-Bzl. The k_{OH}, k_{enz}, and pK_a parameters derived from k_{cat}/K_m values were determined as described in the legend to Fig. 2. The pK_2 values for k_2 and k_3 were not determined due to experimental constraints described below. The k_{cat} parameter does not appear to depend on the ionization of a residue in the *p*H range between 4 and 8. Equation 1 can then be reduced to:

$$k_{cat} = [k_{enz}/1 + (K_2/[H^+])] + [k_{OH}[OH^-]/1 + (K_2/[H^+])]$$

Values for k_{OH} and K_2 can be determined from assays performed at *p*H values of 8 and greater where it is assumed that $k_{OH}[OH^-] >> k_{enz}$. The equation can then be rearranged to the linear form $k_{cat}[H^+] = -K_2k_{cat} + (10^{-14})k_{OH}$. Linear regression analysis of this line with data from assays performed from *p*H 7.96 to 10.18 yields a k_{OH} value of 5.50 ± 0.21 × $10^6 M^{-1}$ min^{-1} and a K_2 value of 5.89 ± 0.50 × $10^{-11} M$. The value of k_{enz} can be estimated from assays performed at *p*H values less than 8 where $[H^+] >> K_2$. By using the k_{OH} value determined above the equation can be reduced to $k_{enz} = k_{cat} - 5.50 \times 10^6[OH^-]$. Subtracting the calculated 5.50 × $10^6[OH^-]$ values from the experimentally derived k_{cat} values from *p*H 4.43 to *p*H 7.33 gives a k_{enz} value of 0.37 ± 0.09 min^{-1}. The *p*H dependence of the acylation rate constant k_2 of the D 102 N trypsin–catalyzed hydrolysis of Z-Lys-S-Bzl was determined by performing assays at 25°C in 50 m*M* Mes, Mops, or Taps buffers, *p*H 4.81 to 8.36 under identical conditions as for assays described in the legend to Fig. 1 except that D 102 N trypsin concentrations (4 to 40 μ*M*) were in large excess over the initial substrate concentration (0.54 μ*M*) and the reaction was allowed to proceed to completion. Assays performed at *p*H values above *p*H 8.4 were too fast to follow spectrophotometrically thereby preventing the determination of k_2 (acylation) values. Values for k_2 and K_m were determined by the procedure of Kezdy and Bender (*28*). The k_{OH} parameter was obtained from a plot of the k_2 values versus solvent hydroxide ion concentration from *p*H 6.70 to 8.36; k_{OH} = 4.91 ± 0.72 × $10^6 M^{-1}$ min^{-1}. Values for k_{enz} and K_1 were obtained by using the k_{OH} value of 4.91 × $10^6 M^{-1}$ min^{-1} and by rearranging Eq. 1 with $[H^+] >> K_2$ to yield:

$$(k_2[H^+] - 4.91 \times 10^{-8})/[H^+] = (1/K_1)(4.91 \times 10^{-8} - k_2[H^+]) + k_{enz}$$

Linear regression analysis of this line with k_2 values determined from assays performed from *p*H 4.81 to *p*H 6.70 yielded a k_{enz} value of 1.32 ± 0.08 min^{-1} and a K_1 value of 5.35 ± 1.00 × $10^{-6} M$. Values for k_3 (deacylation) were calculated using the experimentally derived k_{cat} and k_2 values and the equation: $k_3 = (k_{cat}k_2)/(k_2 - k_{cat})$. The k_{OH} value was determined from a plot of the k_3 values versus solvent hydroxide ion concentration from *p*H 6.70 to 8.36; k_{OH} = 4.57 ± 2.43 × $10^7 M^{-1}$ min^{-1}. The maximal value of the deacylation rate constant of the hydroxide-independent pathway, k_{enz}, was calculated by incorporating the k_{enz} values for k_2 and k_{cat} determined above into the equation $k_3 = k_{cat}$ $k_2/(k_2 - k_{cat})$. This gives a k_{enz} (deacylation) of 0.51 ± 0.07 min^{-1}. The value of k_3 like k_{cat} shows no dependence on the ionization of a residue in the *p*H range between 5 and 8.

Rate constant	k_{OH} (M^{-1} min^{-1})	k_{enz} (min^{-1})	pK_1	pK_2
k_{cat}	5.50 × 10^6	0.37		10.2
k_{cat}/K_m	1.45 × $10^{11} M^{-1}$	4.78 × $10^4 M^{-1}$	5.4	9.9
k_2	4.91 × 10^6	1.32	5.3	
k_3	4.17 × 10^7	0.51		

that approach those of the native enzyme (k_{cat} 6%, k_{cat}/K_m 1%) at *p*H 10.2.

The ascendant alkaline limb of the activity-*p*H profiles of the D 102 N trypsin is not an artifact due to deamidation of the Asn residue to Asp, since mutant enzyme activity at neutral *p*Hs is not affected by preincubation at alkaline *p*H. Furthermore, one would expect the *p*H activity profiles to be similar in shape to those of the naturally occurring enzyme if they merely reflected contamination by trypsin. We ascribe this ascendant basic limb to the participation of a titratable base or bases or of OH^- itself. Although the mechanism of catalysis by the D 102 N trypsin is unknown, the *p*H rate profile of k_{cat}/K_m can be described by a bipartite rate equation in which one part represents the catalytic rate detected at the lower *p*H values and the other part describes the catalytic rate that shows a dependence on hydroxide ion concentration (*19*). The observed rate constant k_{cat}/K_m can be defined as:

$$k_{cat}/K_m = \frac{k_{enz}}{1 + ([H^+]/K_1) + (K_2/[H^+])} + \frac{k_{OH}[OH^-]}{1 + (K_2/[H^+])} \quad (1)$$

where k_{enz} is the rate constant of the hydroxide independent pathway, K_1 and K_2 are the dissociation constants of the ionizing groups, and k_{OH} is the rate constant of the hydroxide ion dependent pathway. The catalytic activity of the OH^--activated and OH^--independent pathways can be resolved with Eq. 1. Values for k_{cat}/K_m determined from mutant enzyme activity studies above *p*H 8.0 show an increase with solvent hydroxide ion concentration that yields k_{OH} and K_2 values of $1.45 \pm 0.12 \times 10^{11} M^{-2}$ min^{-1} and $1.21 \pm 0.30 \times 10^{-10} M$ ($pK_2 = 9.9$), respectively. Between *p*H 8.0 and *p*H 8.8 the k_{cat}/K_m values increase linearly with hydroxide ion concentration. The slight decrease from linearity above *p*H 8.8 may reflect the ionization of another group with an alkaline pK_a value such as the lysine substrate or the amino-terminal group of the protein (*20*).

There is good agreement between the calculated k_{cat}/K_m curve derived from Eq. 1 and the experimentally derived values (Table 2 and Fig. 2). Measurements of k_{cat}/K_m values below *p*H 8.0 yield k_{enz} and K_1 values of $4.78 \pm 0.22 \times 10^4 M^{-1}$ min^{-1} and $3.67 \pm 0.32 \times 10^{-6} M$ ($pK_1 = 5.4$), respectively. A comparison of the k_{enz} value for D 102 N trypsin and the maximal k_{cat}/K_m value for trypsin indicates that the activity of the mutant enzyme (ignoring the contribution of the OH^--dependent pathway) is 25,000 times less than that of trypsin. Thus Asp^{102} is crucial for the catalytic activity at neutral *p*H values. However, the rate of hydrolysis by the mutant enzyme is still 400 times greater than the rate of solvent hydrolysis of the substrate. The inflection points of the curves in Fig. 2 suggests that the pK_a of His^{57} has decreased 1.5 *p*H units in D 102 N trypsin compared to trypsin. The putative alteration in the pK_a value of His^{57} reflects the replacement of the negatively charged carboxylate group with a neutral amide group. The mutant enzyme exhibits classic burst kinetics on ester substrates below *p*H 7.0. This implies that an acyl enzyme intermediate accumulates and that deacylation is rate determining in this *p*H range (*14*).

It has been suggested that Asp^{102} controls the position of the neighboring His^{57} residue that in turn modulates the polarity of the Ser^{195} (*8*). Our demonstration of the crucial role of Asp^{102} is not surprising in view of the strict evolutionary conservation of this residue within the catalytic triad. The magnitude of the catalytic defect from the $Asp^{102} \rightarrow$ Asn replacement and the alkaline activation of the enzyme are unexpected. The three-dimensional structure of D 102 N trypsin is virtually identical to that of trypsin in the alkaline *p*H range (*21*). Thus the activity of the mutant enzyme arises from an active site conformation that resembles the native structure. Certain properties of the D 102 N trypsin superficially resemble chymotrypsin methylated at His^{57} (*22*). The activity of both enzymes is dramatically lower at neutral *p*H values and increases in proportion to OH^- concentration. However, the rate constant ascribed to the reaction with OH^- ions is 1000 times greater for the D 102 N trypsin mutant than for chymotrypsin with the modified histidine. Nevertheless, these results are consistent with the view that compromising the function of the histidine dramatically decreases catalytic activity at neutral *p*H values. This defect can be partly overcome at basic *p*H. The alkaline *p*H may affect the catalytic reaction indirectly by affecting the ionization of groups that function in catalysis. Alternatively, OH^- might participate directly in the reaction; this would require activation at very low hydroxide ion concentrations. The overall catalytic mechanism of the D 102 N trypsin activity is unknown at present. The activity may be due in part to a nucleophilic contribution from the imidazole nitrogen of His^{57} instead of Ser^{195} as has been detected in the cleavage of active esters of nonspecific substrates (*23*). Alternatively, a residue distant from the active site may contribute to stabilization of the tetrahedral intermediate at basic *p*H. Whatever the mechanism of action, D 102 N trypsin displays distinctive properties that distinguish it from trypsin. Its low activity in the neutral *p*H range makes it an unattractive catalyst for most biological functions; thus it might not be expected to persist in evolution. The Asn mutant, however, is of considerable interest as a distinctive serine protease. This work illustrates the potential for creating new variants that are not found in nature because they are active under extreme conditions that are usually incompatible with cellular environments.

REFERENCES AND NOTES

1. J. J. Birktoft and D. M. Blow, *J. Mol. Biol.* **68**, 187 (1972); A. Tulinsky *et al.*, *Biochemistry* **12**, 4185 (1973); R. M. Stroud *et al.*, *J. Mol. Biol.* **83**, 185 (1974); R. Huber *et al.*, *ibid.* **89**, 73 (1974); L. Sawyer *et al.*, *ibid.* **118**, 137 (1978); W. Bode *et al.*, *ibid.* **164**, 237 (1983); C. S. Wright *et al.*, *Nature (London)* **221**, 235 (1969); G. D. Brayer *et al.*, *J. Mol. Biol.* **124**, 261 (1978); P. W. Codding *et al.*, *Can. J. Biochim.* **52**, 208 (1974); G. D. Brayer *et al.*, *J. Mol. Biol.* **131**, 743 (1979).
2. G. H. Dixon, S. Go, H. Neurath, *Biochim. Biophys. Acta* **19**, 193 (1956).
3. E. Shaw, M. Mares-Guia, W. Cohen, *Biochemistry* **4**, 2219 (1965).
4. D. M. Blow, J. J. Birktoft, B. S. Hartley, *Nature (London)* **221**, 337 (1969).
5. W. W. Bachovchin and J. D. Roberts, *J. Am. Chem. Soc.* **100**, 8041 (1978).
6. G. A. Rogers and T. C. Bruice, *ibid.* **96**, 2473 (1974).
7. A. A. Kossiakoff and S. A. Spencer, *Nature (London)* **288**, 414 (1980); J. L. Markley and I. B. Ibanez, *Biochemistry* **22**, 4627 (1978).
8. L. Polgar and M. L. Bender, *Proc. Natl. Acad. Sci. U.S.A.* **64**, 1335 (1969); A. R. Fersht and J. Sperling, *J. Mol. Biol.* **74**, 137 (1973).
9. C. S. Craik *et al.*, *Science* **228**, 291 (1985).
10. M. J. Zoller and M. Smith, *DNA* **3**, 479 (1984).
11. P. J. Southern and P. Berg, *J. Mol. App. Genet.* **4**, 327 (1982).
12. This was accomplished as follows: Chinese hamster ovary cells were co-transfected with a plasmid that contained either the trypsinogen or D 102 N trypsinogen DNA constructs under transcriptional control of the T-antigen early promoter of SV40 and a plasmid that encoded the bacterial phosphotransferase gene (*neo*). The *neo* gene conferred resistance to the amino-glycoside antibiotic G418 and permitted the phenotypic selection of a cell line with high probability of co-expressing the trypsinogen gene. A filter screening assay was developed for detecting high levels of protein secretion from transfected cells in order to isolate cell lines that overproduced trypsinogen (C. S. Craik and R. L. Burke, unpublished results). Cell lines that produced trypsinogens in large amounts (about 10 mg/liter) were then expanded into mass culture (40 liters).
13. J. C. McRae *et al.*, *Biochemistry* **20**, 7196 (1981).
14. C. S. Craik *et al.*, unpublished results.
15. T. Inagami and J. M. Sturtevant, *Biochim. Biophys. Acta* **38**, 64 (1960); H. P. Kasserra and K. J. Laidler, *Can. J. Chem.* **47**, 4021 (1969).
16. The catalysis constant k_{cat} is used as a measure of catalytic activity and is a first-order rate constant that refers to the properties and reactions of the enzyme-substrate, enzyme-intermediate, and enzyme-product complexes. The Michaelis constant K_m relates to the binding affinity of the enzyme for its substrate and is an apparent dissociation constant that may be treated as the overall dissociation constant of all enzyme-bound species. The ratio of k_{cat}/K_m is an apparent second-order rate constant that refers to the properties and reactions of the free enzyme and free substrate (*17*).
17. A. Fersht, *Enzyme Structure and Mechanism* (Freeman, New York, 1985).
18. P. Geneste and M. L. Bender, *Proc. Natl. Acad. Sci. U.S.A.* **64**, 683 (1969).
19. The equation fits the experimental points and suggests a mechanism that involves a combination of an acid HA and OH^-. However, by the principle of kinetic equivalence it cannot be distinguished from a

mechanism involving A^-.
20. M. L. Bender *et al.*, *J. Am. Chem. Soc.* **86**, 3680 (1964); A. Himoe and G. P. Hess, *Biochem. Biophys. Res. Commun.* **23**, 234 (1966).
21. S. Sprang *et al.*, *Science* **237**, 905 (1987).
22. R. Henderson, *Biochem. J.* **124**, 13 (1971); J. Fastrez and N. Houyet, *Eur. J. Biochem.* **81**, 515 (1977).
23. C. D. Hubbard and J. F. Kirsch, *Biochemistry* **11**, 2483 (1972).
24. R. Kitz and F. S. Wilson, *J. Biol. Chem.* **237**, 3245 (1962).
25. Incubations with diisopropylfluorophosphate (DFP) were performed at 25°C with 100 n*M* wild-type or mutant enzyme and varying concentrations of DFP in either 50 m*M* Taps (3-{[tris(hydroxymethyl)methyl]amino} propanesulfonic acid), *p*H 7.96, or 50 m*M* glycine, *p*H 10.03, that contained 0.1*M* NaCl, 1 m*M* $CaCl_2$, 0.005% (w/v) Triton X-100 and 5% (v/v) isopropanol. DFP stock solutions were made up in isopropanol. Final volumes were 0.200 ml and 6.2 ml when incubations were performed with trypsin and D 102 N trypsin, respectively. Trypsin enzyme activities were measured spectrophotometrically at 324 nm by adding 10 μl of the trypsin-DFP solution to 0.99 ml of the same buffer (1 n*M* trypsin final concentration) that contained 60 μ*M* *N*-benzyloxycarbonyl-L-lysine benzylthioester (Z-Lys-S-Bzl) and 250 μ*M* 4,4′-dithiodipyridine but no DFP. Mutant enzyme activities at 324 nm were determined by adding 10 μl of 6 m*M* Z-Lys-S-Bzl and 10 μl of 25 m*M* 4,4′-dithiodipyridine to 0.98 ml of the D 102 N trypsin–DFP solution. The concentrations of DFP during incubations with trypsin at both *p*H values were 0, 20, 25, 40, 80, or 200 μ*M*. In incubations with D 102 N trypsin initial DFP concentrations were 0, 5, 8, 10, or 12.5 m*M*, and 0, 10, 12.5, or 16.6 m*M* when assays were performed at *p*H 7.96 and *p*H 10.03, respectively.
26. T. Yosgimura, L. N. Barker, J. C. Powers, *J. Biol. Chem.* **257**, 5077 (1982).
27. Incubations with tosyl-L-lysine chloromethyl ketone (TLCK) were performed at 25°C with 5 μ*M* unmodified or mutant enzyme in 100 μl of either 100 m*M* Mops [3-*N*(morpholino)propanesulfonic acid], *p*H 7.16 or 100 m*M* Taps, *p*H 8.77, that contained either 0 or 200 μ*M* TLCK. Immediately before assaying trypsin activity an aliquot from the incubation mixtures was diluted 20-fold in 50 m*M* incubation buffer that contained 0.1*M* NaCl, 1 m*M* $CaCl_2$, and 0.005% (w/v) Triton X-100. Ten microliters of the diluted enzyme solution was added to 0.99 ml of the dilution buffer that contained 250 μ*M* 4,4′-dithiodipyridine and 100 μ*M* Z-Lys-S-Bzl (assay buffer); enzyme activities were followed at 25°C spectrophotometrically at 324 nm (2.5 n*M* trypsin). Mutant enzyme activities were determined in an identical manner as described above except that 10 μl of the incubation mixture that contained D 102 N trypsin was added directly to 0.99 ml of the assay buffer (50 n*M* D 102 N trypsin). After 3 hours of incubation with TLCK the loss of catalytic activity of both enzymes at both *p*H values was complete. Since there was no activity of either enzyme after 2.5 hours of further incubation with a large excess of substrate over TLCK, the inhibition was probably due to formation of a covalent bond between the enzyme and the inhibitor and not to a slow-off rate for a noncovalently bound competitive inhibitor.
28. F. J. Kezdy and M. L. Bender, *Biochemistry* **1**, 1097 (1962).
29. Substrate concentrations were calculated by using the total change in absorbance at 324 nm when reactions were run at *p*H 7.5 [ε_{324} = 19,800M^{-1} cm^{-1} (*13*)] and catalyzed by 1 n*M* trypsin so that the reaction would be completed within several minutes. The molar absorptivities over the *p*H range of 4.1 to 10.6 were determined by repeating these reactions with known substrate concentrations at various *p*H values. It was found that at *p*H values below 7.6 the molar absorptivity remained at 19,800M^{-1} cm^{-1}, but that this value decreased sigmoidally above *p*H 7.6, with an apparent pK_a of 8.7, presumably reflecting the ionization of thiopyridine. These molar absorptivity values were used to convert rates of reaction into molar rates at the appropriate *p*H values.

The concentration of viable active sites in native enzyme preparations were determined by active site titrations with 4-methylumbelliferyl *p*-guanidinobenzoate (MUGB) by using 4-methylumbelliferone as a standard (*30*) as described in the legend to Table 1. Titrations of D 102 N trypsin proved to be too slow to measure active sites accurately. Mutant enzyme concentrations were thus determined in duplicate by absorbance at 280 nm (ε_{280} = 38,000M^{-1} cm^{-1}). The accuracy of this molar absorptivity value was confirmed by amino acid analysis with norleucine as an internal standard.

A danger in following the activity of D 102 N trypsin is that an unknown proportion of the activity may be due to trypsin that has formed through deamidation. This does not appear to be a problem at *p*H values less than 8 where the activity of the mutant enzyme is less than 0.1% that of trypsin. At alkaline *p*H values, where the activity of the mutant enzyme becomes significant, the possibility of activity resulting from deamidation becomes greater. However, assays with 100 n*M* D 102 N trypsin and 60 μ*M* Z-Lys-S-Bzl as substrate at *p*H 7.16 and *p*H 10.24 after prior incubation of the enzyme in buffers at either *p*H value for 1 hour gave initial rates of reaction of 1.00 ± 0.04 min^{-1} and 249 ± 5 min^{-1}, respectively. These results indicate that significant deamidation of the D 102 N residue to an aspartic acid did not occur in the *p*H and time ranges studied.
30. G. W. Jameson, D. V. Roberts, R. W. Adams, S. A. Kyle, D. T. Elmore, *Biochem. J.* **131**, 107 (1973).
31. D. V. Roberts, in *Enzyme Kinetics* (Cambridge Univ. Press, Cambridge, 1977), p. 299.
32. K. Yamaoka *et al.*, *J. Pharm. Dyn.* **4**, 879 (1981).
33. We thank J. F. Kirsch and E. T. Kaiser for helpful discussions and L. Spector for preparing the manuscript. Support by NSF grant PCM830610 (W.J.R.) and DMB8608086 (C.S.C.), and a Bristol Meyer grant of Research Corporation (C.S.C.) is gratefully acknowledged. An NIH postdoctoral fellowship was awarded to S.R. (GM 10765).

29 September 1986; accepted 29 May 1987

Adrenal Medulla Grafts Enhance Recovery of Striatal Dopaminergic Fibers

MARTHA C. BOHN,* LISA CUPIT, FREDERICK MARCIANO, DON M. GASH

The drug, 1-methyl-4-phenyl-1,2,5,6-tetrahydropyridine (MPTP), depletes striatal dopamine levels in primates and certain rodents, including mice, and produces parkinsonian-like symptoms in humans and nonhuman primates. To investigate the consequences of grafting adrenal medullary tissue into the brain of a rodent model of Parkinson's disease, a piece of adult mouse adrenal medulla was grafted unilaterally into mouse striatum 1 week after MPTP treatment. This MPTP treatment resulted in the virtual disappearance of tyrosine hydroxylase–immunoreactive fibers and severely depleted striatal dopamine levels. At 2, 4, and 6 weeks after grafting, dense tyrosine hydroxylase–immunoreactive fibers were observed in the grafted striatum, while only sparse fibers were seen in the contralateral striatum. In all cases, tyrosine hydroxylase–immunoreactive fibers appeared to be from the host rather than from the grafts, which survived poorly. These observations suggest that, in mice, adrenal medullary grafts exert a neurotrophic action in the host brain to enhance recovery of dopaminergic neurons. This effect may be relevant to the symptomatic recovery in Parkinson's disease patients who have received adrenal medullary grafts.

IN HUMANS, THE DRUG, 1-METHYL-4-phenyl-1,2,5,6-tetrahydropyridine (MPTP), produces motor deficits that closely resemble those observed in Parkinson's disease (*1–4*). This observation has led to the development of animal models of Parkinson's disease that are valuable for studying the effects of brain grafting (*5*). MPTP damages the dopamine (DA)-containing A9 cell group in the pars compacta of the substantia nigra and results in a degeneration of the nigrostriatal DA fibers and loss of striatal DA and its metabolites (*1–8*). The severity of this damage is species-dependent. In primates, MPTP treatment damages both the DA fibers and cell bodies (*1–5*). In mice, the fibers are damaged, but many A9 neurons survive (*6, 7*). Because the MPTP lesion is transient in mouse (*7, 9*), the MPTP-treated mouse provides an opportunity for studying recovery of identified neurons in the brain. Our study suggests that striatal grafts of adult mouse adrenal medulla enhance recovery of these neurons.

Two MPTP treatments were compared for their effects on striatal DA levels and tyrosine hydroxylase–immunoreactivity (TH-IR) in the striatum and A9 region of C57BL/6 mice (6 to 12 weeks old; 21 to 28 g). As described (*6, 7*), lightly etherized mice received multiple injections of MPTP·HCl subcutaneously in 0.5 ml of saline. Group A received three injections of 30 mg per kilogram of body weight at 24-hour intervals and group B received two injections of 50 mg per kilogram of body weight 16 hours apart. Catecholamines in tissues were isolated and measured

M. C. Bohn and L. Cupit, Department of Neurobiology and Behavior, State University of New York, Stony Brook, NY 11794.
F. Marciano and D. M. Gash, Department of Neurobiology and Anatomy, University of Rochester School of Medicine, Rochester, NY 14642.

*To whom correspondence should be addressed.